

The measurable impact of the 2pN spin-dependent accelerations on the jet precession of M87*

Lorenzo Iorio 

Ministero dell' Istruzione e del Merito
 Viale Unità di Italia 68, I-70125, Bari, Italy
 email: lorenzo.iorio@libero.it

February 12, 2026

Abstract

Motivated by recent accurate measurements of disk/jet coprecessions around some galactic supermassive black holes, the accelerations experienced by an uncharged, spinless object in the Kerr metric, written in harmonic coordinates, are analytically calculated up to the formal second post-Newtonian order. To such a level, some new accelerations make their appearance. They are proportional to even and odd powers of the hole's angular momentum. Their counterparts are not known where the primary is a material body. After expressing them in a coordinate-independent, vector form valid for any orientations of the hole's spin axis in space, their orbital effects are perturbatively worked out in terms of the particle's Keplerian orbital elements. The resulting expressions, averaged over one orbital revolution, are valid for generic shapes and inclinations of the orbit. The orbital plane's precession proportional to the first power of the hole's angular momentum and to the reciprocal of the fourth power of the speed of light amounts to about twenty per cent of the corresponding Lense-Thirring effect. The latter is believed to be the cause of the accurately measured disk/jet precessional phenomenology, currently measured to a few per cent accuracy. Although at a lesser extent, also the precession proportional to the second power of the hole's spin and to the reciprocal of the fourth power of the speed of light is measurable. Allowed domains in the parameter space of the jet precession around M87* are displayed.

keywords— Gravitation (661); Celestial mechanics (211); Black holes (162)

1 Introduction

Recently, the precessions of both the jet and the accretion disk around some supermassive black holes—or megaplyknons-lurking in galactic nuclei were measured to a per cent accuracy. In particular, the jet precession around M87* was measured to $\simeq 3\%$ (Cui et al., 2023), while the disk/jet coprecession associated with the tidal disruption event AT2020afhd was detected to $\simeq 7\%$ (Wang et al., 2025). In both scenarios, the jet and the accretion disk were considered tightly coupled. Furthermore, the latter one was assumed misaligned with respect to the hole's equator.

It was demonstrated that such precessional phenomenology can be successfully explained in terms of the Lense-Thirring effect, which is formally of the first post-Newtonian (1pN) order, changing the orbital angular momentum of a fictitious test particle orbiting the black hole—or pyknon—at hand along a circular orbit whose effective radius amounts approximately to ten and a half gravitational radii (Iorio, 2025).

Given the good experimental accuracies already reached so far and in view of further improvements expected in the next future, the success of the aforementioned effective test particle scheme demands to accurately investigate all the accelerations that can cause the orbital plane of a fictitious nonspinning and uncharged body to precess in the Kerr spacetime to higher pN orders than done until now. To this aim and to facilitate the interpretation of the observations avoiding spurious coordinate artifacts, the Kerr metric will be written in harmonic coordinates, and the geodesic equations of motion of a test particle will be analyzed formally up to the 2pN order. General expressions for the resulting accelerations, expanded up to the fourth power of the hole's spin S , will be obtained without restricting to the hole's equatorial plane which, moreover, will be assumed arbitrarily oriented in space. Their orbital effects, averaged over one orbital revolution, will be calculated for general shapes and inclinations of the particle's orbit.

The accelerations will be expressed in a coordinate-independent, vector form, while their orbital effects will be calculated in terms of the standard Keplerian orbital elements in order to make them accessible to the widest possible readership, especially to those acquainted with the widely used formalism of celestial mechanics and dynamical astronomy. These distinctive features make it difficult to straightforwardly compare the present results with others that can be found in the literature. Indeed, the latter ones were often obtained by using more abstract formalisms. Last but not least, the order of approximation to which they were obtained is lower than the present one; see, e.g., [Hergt et al. \(2013\)](#) and [Porto and Rothstein \(2008\)](#), and references therein.

In addition to some well known accelerations like the 1pN and 2pN mass-only ones, the formally 1pN Lense-Thirring acceleration proportional to¹ S/c^2 , where c is the speed of light in vacuum, the formally² ‘Newtonian’ accelerations due to the first two even zonal mass multipoles accounting for the axisymmetric departures from spherically symmetry of the primary and the formally³ 1pN quadrupolar acceleration, also other less known-if any-accelerations, proportional to S^k/c^4 , $k = 1, 2, 3$, will be obtained.

The paper is organized as follows. The transformation of the Kerr metric from the Boyer-Lindquist coordinates to the harmonic ones is performed in Section 2. The resulting accelerations are discussed in Section 3. Section 4 deals with the perturbative calculational scheme to work out their orbital effects. Those of the order of $\mathcal{O}(S/c^4)$ are treated in Section 5. Section 6 is devoted to the consequences of the position-dependent acceleration of the order of $\mathcal{O}(S^2/c^4)$. The calculation of the impact of the acceleration of the order of $\mathcal{O}(S^3/c^4)$ is presented in Section 7. In Section 8, the results obtained in the previous Sections are applied to the M87* scenario by obtaining allowed regions in the two-dimensional spin-orbit radius parameter space suitable for it. Section 9 summarizes the findings and offers conclusions.

2 The Kerr metric in harmonic coordinates

The squared spacetime interval $(ds)^2$ of the Kerr metric, written in terms of the Boyer-Lindquist coordinates $x_{\text{BL}}^0, r_{\text{BL}}, \theta_{\text{BL}}, \phi_{\text{BL}}$ in a reference frame whose fundamental plane is aligned with the hole's equator, is

$$(ds)^2 = g_{00}^{\text{BL}} \left(dx_{\text{BL}}^0 \right)^2 + 2g_{0\phi}^{\text{BL}} dx_{\text{BL}}^0 d\phi_{\text{BL}} + g_{rr}^{\text{BL}} (dr_{\text{BL}})^2 + g_{\theta\theta}^{\text{BL}} (d\theta_{\text{BL}})^2 + g_{\phi\phi}^{\text{BL}} (d\phi_{\text{BL}})^2. \quad (1)$$

¹For a Kerr black hole, it is of the order of $\mathcal{O}(1/c^3)$.

²For a Kerr black hole, they are of the order of $\mathcal{O}(1/c^4)$ and $\mathcal{O}(1/c^8)$, respectively.

³For a Kerr black hole, it is of the order of $\mathcal{O}(1/c^6)$.

The spacetime metric coefficients $g_{\mu\nu}^{\text{BL}}$ entering Equation (1) can be cast into the form⁴ (Hergt and Schäfer, 2008)

$$g_{00}^{\text{BL}} = \frac{a_g^2 \sin^2 \theta_{\text{BL}} - \Delta}{\rho^2}, \quad (2)$$

$$g_{rr}^{\text{BL}} = \frac{\rho^2}{\Delta}, \quad (3)$$

$$g_{\theta\theta}^{\text{BL}} = \rho^2, \quad (4)$$

$$g_{\phi\phi}^{\text{BL}} = \frac{\sin^2 \theta_{\text{BL}}}{\rho^2} \left[(r_{\text{BL}}^2 + a_g^2)^2 - a_g^2 \Delta \sin^2 \theta_{\text{BL}} \right], \quad (5)$$

$$g_{0\phi}^{\text{BL}} = \frac{\sin^2 \theta_{\text{BL}}}{\rho^2} \left[a_g \Delta - a_g (r_{\text{BL}}^2 + a_g^2) \right]. \quad (6)$$

In Equations (2)–(6), it is

$$\rho^2 := r_{\text{BL}}^2 + a_g^2 \cos^2 \theta_{\text{BL}}, \quad (7)$$

$$\Delta := r_{\text{BL}}^2 - 2R_g r_{\text{BL}} + a_g^2. \quad (8)$$

The dimensional parameters R_g and a_g entering Equations (2)–(8) are defined as⁵

$$R_g := \frac{GM}{c^2}, \quad (9)$$

$$a_g := \frac{S}{Mc}, \quad (10)$$

where G and c are the Newtonian constant of gravitation and the speed of light in a vacuum, while M and S are the hole's mass and spin, respectively. Both Equation (9) and Equation (10) are dimensionally lengths, with Equation (9) being nothing else the hole's gravitational radius.

For the purpose of the present paper, it is convenient to express the Kerr metric in terms of the harmonic coordinates, which will be labeled as x^0, r, θ, ϕ in the following. This can be done starting

⁴In the coefficient of $d\phi_B^2$ of Equation (69) in Hergt and Schäfer (2008) there is a typo: $(r_B^2 + a^2)$ should be replaced by its squared counterpart $(r_B^2 + a^2)^2$; here, it is meant that $d\phi_B \rightarrow d\phi_{\text{BL}}$, $r_B \rightarrow r_{\text{BL}}$ and $a \rightarrow a_g$ of the present notation.

⁵The spin parameter a_g should not be confused with the semimajor axis of the orbit of the test particle which is customarily denoted as a in celestial mechanics.

from (Hergt and Schäfer, 2008)

$$x^0 = x_{\text{BL}}^0, \quad (11)$$

$$x + iy = (r_{\text{BL}} - R_g + ia_g) e^{i\xi_{\text{BL}}} \sin \theta_{\text{BL}}, \quad (12)$$

$$r^2 = (r_{\text{BL}} - R_g)^2 + a_g^2 \sin^2 \theta_{\text{BL}}, \quad (13)$$

$$r^2 \cos^2 \theta = (r_{\text{BL}} - R_g)^2 \cos^2 \theta_{\text{BL}}. \quad (14)$$

In Equation (12),

$$x = r \sin \theta \cos \phi, \quad (15)$$

$$y = r \sin \theta \sin \phi \quad (16)$$

are the harmonic Cartesian coordinates,

$$i := \sqrt{-1} \quad (17)$$

is the imaginary unit, and

$$\xi_{\text{BL}} := \phi_{\text{BL}} + \frac{a_g}{r_+ - r_-} \ln \left| \frac{r_{\text{BL}} - r_+}{r_{\text{BL}} - r_-} \right|, \quad (18)$$

where

$$r_{\pm} := R_g \pm \sqrt{R_g^2 - a_g^2}. \quad (19)$$

In the Kerr metric, r_{\pm} range within

$$R_g \leq r_+ \leq 2R_g, \quad (20)$$

$$0 \leq r_- \leq R_g. \quad (21)$$

Since in the scenario of interest here the test particle stays far from the event horizon, $r_{\text{BL}} > r_{\pm}$, and the absolute value in Equation (18) can be dropped in the following.

From Equations (13)–(14), two solutions for $\sin^2 \theta_{\text{BL}}$ can be obtained in terms of the harmonic coordinates r and θ . They are

$$\sin^2 \theta_{\text{BL}} = \frac{a_g^2 + r^2 \mp \sqrt{\mathcal{B}_1}}{2a_g^2}, \quad (22)$$

where

$$\mathcal{B}_1 := a_g^4 + r^4 + 2a_g^2 r^2 \cos 2\theta. \quad (23)$$

Only the one with the minus sign has to be retained since it is finite in the limit $a_g \rightarrow 0$, contrary to the one with the plus sign which, instead, diverges. Thus, it is

$$\sin^2 \theta_{\text{BL}} = \frac{a_g^2 + r^2 - \sqrt{\mathcal{B}_1}}{2a_g^2}, \quad (24)$$

$$\cos^2 \theta_{\text{BL}} = \frac{a_g^2 - r^2 + \sqrt{\mathcal{B}_1}}{2a_g^2}; \quad (25)$$

note that both $\sin^2 \theta_{\text{BL}}$ and $\cos^2 \theta_{\text{BL}}$ enter explicitly Equations (2)–(7). In the limit $a_g \rightarrow 0$, Equations (24)–(25) reduce to

$$\sin^2 \theta_{\text{BL}} \rightarrow \sin^2 \theta, \quad (26)$$

$$\cos^2 \theta_{\text{BL}} \rightarrow \cos^2 \theta. \quad (27)$$

From Equations (24)–(25), the differential $d\theta_{\text{BL}}$, entering explicitly Equation (1), can be obtained in terms of $r, \theta, dr, d\theta$ as

$$d\theta_{\text{BL}} = \frac{(-r^2 - a_g^2 \cos 2\theta + \sqrt{\mathcal{B}_1}) dr + a_g^2 r \sin 2\theta d\theta}{\sqrt{2\mathcal{B}_1 (-r^2 - a_g^2 \cos 2\theta + \sqrt{\mathcal{B}_1})}}. \quad (28)$$

From Equation (13), calculated with Equation (24), the following two solutions for r_{BL} , which enters explicitly Equations (2)–(8), can be obtained in terms of the harmonic coordinates r and θ :

$$r_{\text{BL}} = R_g \mp \sqrt{\frac{r^2 - a_g^2 + \sqrt{\mathcal{B}_1}}{2}}. \quad (29)$$

Only the solution with the plus sign is acceptable since, in the limit $a_g \rightarrow 0$, it reduces to

$$r_{\text{BL}} \rightarrow R_g + r, \quad (30)$$

while the one with the minus sign would lead to

$$r_{\text{BL}} \rightarrow R_g - r < 0 \quad (31)$$

for $r > R_g$, as in the present case. Thus, from

$$r_{\text{BL}} = R_g + \sqrt{\frac{r^2 - a_g^2 + \sqrt{\mathcal{B}_1}}{2}} \quad (32)$$

the differential dr_{BL} , entering explicitly Equation (1), can be obtained in terms of $r, \theta, dr, d\theta$. It reads

$$dr_{\text{BL}} = \frac{r(\sqrt{\mathcal{B}_1} + r^2 + a_g^2 \cos 2\theta) dr - a_g^2 r^2 \sin 2\theta d\theta}{\sqrt{2\mathcal{B}_1 (r^2 - a_g^2 + \sqrt{\mathcal{B}_1})}}. \quad (33)$$

Finally, from Equation (12), Equations (15)–(16) and Equations (18)–(19), the differential $d\phi_{\text{BL}}$, which enters explicitly Equation (1), contrary to ϕ_{BL} itself, can be obtained in terms of $r, \theta, dr, d\theta$. It is

$$d\phi_{\text{BL}} = \frac{\sqrt{2} a_g R_g^2 r [(r^2 + a_g^2 \cos 2\theta + \sqrt{\mathcal{B}_1}) dr + a_g^2 r \sin 2\theta d\theta]}{\sqrt{\mathcal{B}_1} \sqrt{-a_g^2 + r^2 + \sqrt{\mathcal{B}_1}} \{a_g^4 - R_g^2 r^2 + r^4 + a_g^2 [-R_g^2 + 2r^2 \cos^2 \theta] + (a_g^2 - R_g^2 + r^2) \sqrt{\mathcal{B}_1}\}}. \quad (34)$$

By calculating Equations (1)–(8) with Equations (24)–(25), Equations (28)–(29), and Equations (33)–(34) it is possible to express the spacetime metric tensor $g_{\mu\nu}$ of the Kerr metric in terms of the harmonic

coordinates. It turns out that it is fully non-diagonal since all its off-diagonal coefficients are nonvanishing. The resulting exact expressions for $g_{\mu\nu}$ are

$$g_{00} = \frac{R_g^2 - \sqrt{\mathcal{B}_1}}{\sqrt{\mathcal{B}_1} + R_g \left(R_g + \sqrt{2} \sqrt{-a_g^2 + \sqrt{\mathcal{B}_1} + r^2} \right)}, \quad (35)$$

$$\begin{aligned} g_{rr} = & \frac{(\sqrt{\mathcal{B}_1} - r^2) \left[\sqrt{\mathcal{B}_1} + R_g \left(R_g + \sqrt{2} \sqrt{-a_g^2 + \sqrt{\mathcal{B}_1} + r^2} \right) \right]}{2\mathcal{B}_1} + \\ & + \frac{1}{2\mathcal{B}_1^{3/2} (-a_g^2 + \sqrt{\mathcal{B}_1} + r^2)^{3/2} (a_g^2 + \sqrt{\mathcal{B}_1} - 2R_g^2 + r^2)} \left[-\sqrt{2} a_g^2 R_g + \sqrt{2} R_g (\sqrt{\mathcal{B}_1} + r^2) + \right. \\ & \left. + \sqrt{\mathcal{B}_1} \sqrt{-a_g^2 + \sqrt{\mathcal{B}_1} + r^2} + R_g^2 \sqrt{-a_g^2 + \sqrt{\mathcal{B}_1} + r^2} \right] \left\{ a_g^2 \left[(a_g^2 - \sqrt{\mathcal{B}_1}) \sqrt{\mathcal{B}_1} (a_g^2 + \sqrt{\mathcal{B}_1} - 2R_g^2) + \right. \right. \\ & \left. \left. + 2(2a_g^4 - \mathcal{B}_1 + \sqrt{\mathcal{B}_1} R_g^2) r^2 + 7\sqrt{\mathcal{B}_1} r^4 + 12r^6 \right] \cos 2\theta + r^2 \left[4r^4 (\sqrt{\mathcal{B}_1} + r^2) + \right. \right. \\ & \left. \left. + a_g^4 (3\sqrt{\mathcal{B}_1} + 8r^2) + a_g^4 (\sqrt{\mathcal{B}_1} + 4r^2) \cos 4\theta \right] \right\} + \frac{1}{\mathcal{B}_2} \left\{ R_g^4 r^2 (a_g^2 - \sqrt{\mathcal{B}_1} + r^2) \left[4r^4 (\sqrt{\mathcal{B}_1} + r^2) + \right. \right. \\ & \left. \left. + a_g^4 (3\sqrt{\mathcal{B}_1} + 8r^2) + 4a_g^2 (a_g^4 + 2\sqrt{\mathcal{B}_1} r^2 + 3r^4) \cos 2\theta + a_g^4 (\sqrt{\mathcal{B}_1} + 4r^2) \cos 4\theta \right] \right\} \times \\ & \times \left\{ 3a_g^2 + \sqrt{\mathcal{B}_1} + r^2 + \frac{8\sqrt{2} R_g (a_g^2 + R_g^2)}{\sqrt{-a_g^2 + \sqrt{\mathcal{B}_1} + r^2}} + 4R_g \left(3R_g + \sqrt{2} \sqrt{-a_g^2 + \sqrt{\mathcal{B}_1} + r^2} \right) + \right. \\ & \left. + \frac{2 \left[2a_g^4 + a_g^2 (5R_g^2 - r^2) + R_g^2 (-\sqrt{\mathcal{B}_1} + 2R_g^2 + r^2) + a_g^2 r^2 \cos 2\theta \right]}{-a_g^2 + \sqrt{\mathcal{B}_1} + r^2} \right\}, \quad (36) \end{aligned}$$

$$\begin{aligned} g_{\theta\theta} = & \frac{1}{2\mathcal{B}_1 (-a_g^2 + \sqrt{\mathcal{B}_1} + r^2)^{3/2} (a_g^2 + \sqrt{\mathcal{B}_1} - 2R_g^2 + r^2) (\sqrt{\mathcal{B}_1} - r^2 - a_g^2 \cos 2\theta)} \times \\ & \times a_g^4 r^2 \left\{ \sqrt{\mathcal{B}_1} \sqrt{-a_g^2 + \sqrt{\mathcal{B}_1} + r^2} + R_g \left[R_g \sqrt{-a_g^2 + \sqrt{\mathcal{B}_1} + r^2} + \sqrt{2} (-a_g^2 + \sqrt{\mathcal{B}_1} + r^2) \right] \right\} \times \\ & \times \left[-a_g^4 + \mathcal{B}_1 + 2a_g^2 R_g^2 - 2\sqrt{\mathcal{B}_1} (R_g^2 - 2r^2) - r^2 (2R_g^2 + r^2) - 2a_g^2 r^2 \cos 2\theta \right] \sin^2 \theta + \end{aligned}$$

$$\begin{aligned}
& + \frac{1}{\mathcal{B}_3} \left[a_g^4 R_g^4 r^4 (a_g^2 - \sqrt{\mathcal{B}_1} + r^2) \left\{ \sqrt{-a_g^2 + \sqrt{\mathcal{B}_1} + r^2} [a_g^4 + \mathcal{B}_1 + 4R_g^4 + 2a_g^2 (\sqrt{\mathcal{B}_1} - R_g^2) + \right. \right. \\
& + 14R_g^2 r^2 + r^4 + 2\sqrt{\mathcal{B}_1} (5R_g^2 + r^2) + 2a_g^2 r^2 \cos 2\theta] + \\
& \left. \left. + 4\sqrt{2}R_g (-a_g^2 + \sqrt{\mathcal{B}_1} + r^2) (a_g^2 + \sqrt{\mathcal{B}_1} + 2R_g^2 + r^2) \right\} \sin^2 2\theta \right], \tag{37}
\end{aligned}$$

$$\begin{aligned}
g_{\phi\phi} = & \frac{a_g^2 - \sqrt{\mathcal{B}_1} + r^2}{8a_g^2 \left[\sqrt{\mathcal{B}_1} + R_g \left(R_g + \sqrt{2} \sqrt{-a_g^2 + \sqrt{\mathcal{B}_1} + r^2} \right) \right]} \left\{ a_g^4 + \mathcal{B}_1 + 4R_g^4 + 14R_g^2 r^2 + r^4 + \right. \\
& + 4\sqrt{2}R_g (2R_g^2 + r^2) \sqrt{-a_g^2 + \sqrt{\mathcal{B}_1} + r^2} + 2\sqrt{\mathcal{B}_1} \left(5R_g^2 + r^2 + 2\sqrt{2}R_g \sqrt{-a_g^2 + \sqrt{\mathcal{B}_1} + r^2} \right) + \\
& \left. + 2a_g^2 \left[\sqrt{\mathcal{B}_1} + R_g \left(-R_g + 2\sqrt{2} \sqrt{-a_g^2 + \sqrt{\mathcal{B}_1} + r^2} \right) \right] + 2a_g^2 r^2 \cos 2\theta \right\}, \tag{38}
\end{aligned}$$

$$g_{0r} = \frac{R_g^3 r (a_g^2 - \sqrt{\mathcal{B}_1} + r^2) (2R_g + \sqrt{2} \sqrt{-a_g^2 + \sqrt{\mathcal{B}_1} + r^2}) (\sqrt{\mathcal{B}_1} + r^2 + a_g^2 \cos 2\theta)}{\mathcal{B}_4}, \tag{39}$$

$$g_{0\theta} = -\frac{a_g^2 R_g^3 r^2 (a_g^2 - \sqrt{\mathcal{B}_1} + r^2) (2R_g + \sqrt{2} \sqrt{-a_g^2 + \sqrt{\mathcal{B}_1} + r^2}) \sin 2\theta}{\mathcal{B}_4}, \tag{40}$$

$$g_{0\phi} = -\frac{R_g (a_g^2 - \sqrt{\mathcal{B}_1} + r^2) (2R_g + \sqrt{2} \sqrt{-a_g^2 + \sqrt{\mathcal{B}_1} + r^2})}{2a_g \left[\sqrt{\mathcal{B}_1} + R_g \left(R_g + \sqrt{2} \sqrt{-a_g^2 + \sqrt{\mathcal{B}_1} + r^2} \right) \right]}, \tag{41}$$

$$\begin{aligned}
g_{r\theta} = & -\frac{a_g^2 R_g^2 r \left[\sqrt{\mathcal{B}_1} + R_g \left(R_g + \sqrt{2} \sqrt{-a_g^2 + \sqrt{\mathcal{B}_1} + r^2} \right) \right] \sin 2\theta}{\mathcal{B}_1 (a_g^2 + \sqrt{\mathcal{B}_1} - 2R_g^2 + r^2)} - \\
& - \frac{a_g^2 R_g^4 r^3 (a_g^2 - \sqrt{\mathcal{B}_1} + r^2) [a_g^4 + \sqrt{\mathcal{B}_1} r^2 + r^4 + a_g^2 (\sqrt{\mathcal{B}_1} + 2r^2) \cos 2\theta]}{\mathcal{B}_5} \times \\
& \times \left\{ \left[a_g^2 + \frac{1}{4} \left(2R_g + \sqrt{2} \sqrt{-a_g^2 + \sqrt{\mathcal{B}_1} + r^2} \right)^2 \right]^2 + \right. \tag{42}
\end{aligned}$$

$$+ \frac{1}{2} \left[a_g^2 (R_g^2 - r^2) + R_g^2 (-\sqrt{\mathcal{B}_1} + r^2) + a_g^2 r^2 \cos 2\theta \right] \} \sin 2\theta, \quad (42)$$

$$g_{r\phi} = -\frac{R_g^2 r (a_g^2 - \sqrt{\mathcal{B}_1} + r^2) (\sqrt{\mathcal{B}_1} + r^2 + a_g^2 \cos 2\theta)}{a_g H} \times \\ \times \left\{ \left[a_g^2 + \frac{1}{4} \left(2R_g + \sqrt{2} \sqrt{-a_g^2 + \sqrt{\mathcal{B}_1} + r^2} \right)^2 \right]^2 + \frac{1}{2} \left[a_g^2 (R_g^2 - r^2) + R_g^2 (-\sqrt{\mathcal{B}_1} + r^2) + a_g^2 r^2 \cos 2\theta \right] \right\}, \quad (43)$$

$$g_{\theta\phi} = \frac{a_g R_g^2 r^2 (a_g^2 - \sqrt{\mathcal{B}_1} + r^2)}{\mathcal{B}_4} \left\{ \left[a_g^2 + \frac{1}{4} \left(2R_g + \sqrt{2} \sqrt{-a_g^2 + \sqrt{\mathcal{B}_1} + r^2} \right)^2 \right]^2 + \right. \\ \left. + \frac{1}{2} \left[a_g^2 (R_g^2 - r^2) + R_g^2 (-\sqrt{\mathcal{B}_1} + r^2) + a_g^2 r^2 \cos 2\theta \right] \right\} \sin 2\theta. \quad (44)$$

The auxiliary functions $\mathcal{B}_2, \mathcal{B}_3, \mathcal{B}_4, \mathcal{B}_5$ of r, θ and a_g, R_g which were introduced in Equations (35)–(44) are

$$\mathcal{B}_2 := 8\mathcal{B}_1^{3/2} \left[\sqrt{\mathcal{B}_1} + R_g \left(R_g + \sqrt{2} \sqrt{-a_g^2 + \sqrt{\mathcal{B}_1} + r^2} \right) \right] \times \\ \times \left[(a_g^2 + \sqrt{\mathcal{B}_1}) (a_g^2 - R_g^2) + (a_g^2 + \sqrt{\mathcal{B}_1} - R_g^2) r^2 + r^4 + a_g^2 r^2 \cos 2\theta \right]^2, \quad (45)$$

$$\mathcal{B}_3 := 4 (-a_g^2 + \sqrt{\mathcal{B}_1} + r^2)^{3/2} \left[\mathcal{B}_1^{3/2} + \mathcal{B}_1 R_g \left(R_g + \sqrt{2} \sqrt{-a_g^2 + \sqrt{\mathcal{B}_1} + r^2} \right) \right] \times \\ \times \left[(a_g^2 + \sqrt{\mathcal{B}_1}) (a_g^2 - R_g^2) + (a_g^2 + \sqrt{\mathcal{B}_1} - R_g^2) r^2 + r^4 + a_g^2 r^2 \cos 2\theta \right]^2, \quad (46)$$

$$\mathcal{B}_4 := \sqrt{2\mathcal{B}_1} \sqrt{-a_g^2 + \sqrt{\mathcal{B}_1} + r^2} \left[\sqrt{\mathcal{B}_1} + R_g \left(R_g + \sqrt{2} \sqrt{-a_g^2 + \sqrt{\mathcal{B}_1} + r^2} \right) \right] \times \\ \times \left[(a_g^2 + \sqrt{\mathcal{B}_1}) (a_g^2 - R_g^2) + (a_g^2 + \sqrt{\mathcal{B}_1} - R_g^2) r^2 + r^4 + a_g^2 r^2 \cos 2\theta \right], \quad (47)$$

$$\mathcal{B}_5 := \mathcal{B}_1^{3/2} (-a_g^2 + \sqrt{\mathcal{B}_1} + r^2) \left(\sqrt{\mathcal{B}_1} + R_g^2 + \sqrt{2} R_g \sqrt{-a_g^2 + \sqrt{\mathcal{B}_1} + r^2} \right) \times \\ \times \left[a_g^4 - R_g^2 r^2 + r^4 + a_g^2 (-R_g^2 + r^2) + \sqrt{\mathcal{B}_1} (a_g^2 - R_g^2 + r^2) + a_g^2 r^2 \cos 2\theta \right]^2. \quad (48)$$

By expanding Equations (35)–(44) in powers of a_g and R_g , it is possible to obtain approximate expressions for them in agreement with those of Equations (80)–(83) in [Hergt and Schäfer \(2008\)](#). In the

following, the power expansion will be pushed beyond the order strictly required to match the results by [Hergt and Schäfer \(2008\)](#) in order to fully capture the accelerations of the order of $O(1/c^4)$, as shown in the next Section.

3 The geodesic equations of motion of a test particle

The next step consists of calculating the geodesic equations of motion for the test particle to the desired order of approximation in inverse powers of c . Written in terms of the coordinate time $t = x^0/c$, they are ([Soffel and Han, 2019](#))

$$\ddot{x}^i = -c^2 \left[\Gamma_{00}^i + 2\Gamma_{0j}^i \frac{\dot{x}^j}{c} + \Gamma_{jk}^i \frac{\dot{x}^j}{c} \frac{\dot{x}^k}{c} - \left(\Gamma_{00}^0 + 2\Gamma_{0j}^0 \frac{\dot{x}^j}{c} + \Gamma_{jk}^0 \frac{\dot{x}^j}{c} \frac{\dot{x}^k}{c} \right) \frac{\dot{x}^i}{c} \right], \quad i = 1, 2, 3 \quad (49)$$

where

$$\dot{x}^i := \frac{dx^i}{dt}, \quad i = 1, 2, 3, \quad (50)$$

$$\ddot{x}^i := \frac{d^2 x^i}{dt^2}, \quad i = 1, 2, 3, \quad (51)$$

and $\Gamma_{\beta\gamma}^\alpha$ are the Christoffel symbols of the second kind defined as

$$\Gamma_{\beta\gamma}^\alpha := \frac{1}{2} g^{\rho\alpha} \left(\frac{\partial g_{\beta\rho}}{\partial x^\gamma} + \frac{\partial g_{\gamma\rho}}{\partial x^\beta} - \frac{\partial g_{\beta\gamma}}{\partial x^\rho} \right), \quad \alpha, \beta, \gamma = 0, 1, 2, 3. \quad (52)$$

In Equation (52), $g^{\mu\nu}$ is the inverse metric tensor.

As far as the coordinates x^i , $i = 1, 2, 3$ and their time derivatives entering Equation (49) are concerned, in the present case it is

$$x^1 = r, \quad (53)$$

$$x^2 = \theta, \quad (54)$$

$$x^3 = \phi, \quad (55)$$

$$\dot{x}^1 = \dot{r}, \quad (56)$$

$$\dot{x}^2 = \dot{\theta}, \quad (57)$$

$$\dot{x}^3 = \dot{\phi}, \quad (58)$$

$$\ddot{x}^1 = \ddot{r}, \quad (59)$$

$$\ddot{x}^2 = \ddot{\theta}, \quad (60)$$

$$\ddot{x}^3 = \ddot{\phi}. \quad (61)$$

It may be useful to recall that, in spherical coordinates, the components of the velocity and acceleration are

$$v_r = \dot{r}, \quad (62)$$

$$v_\theta = r\dot{\theta}, \quad (63)$$

$$v_\phi = r \sin \theta \dot{\phi} \quad (64)$$

and

$$A_r = \ddot{r} - r(\dot{\theta}^2 + \sin^2 \theta \dot{\phi}^2), \quad (65)$$

$$A_\theta = r\ddot{\theta} + 2\dot{r}\dot{\theta} - r \sin \theta \cos \theta \dot{\phi}^2, \quad (66)$$

$$A_\phi = r \sin \theta \ddot{\phi} + 2\dot{\phi} (r \cos \theta \dot{\theta} + \sin \theta \dot{r}), \quad (67)$$

respectively. The full expressions of the Christoffel symbols for the Kerr metric in harmonic coordinates cannot be explicitly displayed here because of their extreme cumbersomeness.

A computationally efficient way to proceed consists of calculating Equation (49) starting from suitably approximated expressions of Equations (35)–(44) and expanding the result to the desired order in inverse powers of c . In the following, the terms of the order of $O(1/c^2)$ and $O(1/c^4)$ will be considered.

Following the aforementioned approach, Equation (49) yields

$$A_r \simeq -\frac{GM}{r^2} + A_r^{(1/c^2)} + A_r^{(1/c^4)}, \quad (68)$$

$$A_\theta \simeq A_\theta^{(1/c^2)} + A_\theta^{(1/c^4)}, \quad (69)$$

$$A_\phi \simeq A_\phi^{(1/c^2)} + A_\phi^{(1/c^4)} \quad (70)$$

3.1 The accelerations of the order of $O(1/c^2)$

In Equations (68)–(70), there are three terms which are formally of the order of $O(1/c^2)$. They turn out to be the standard Schwarzschild-like acceleration due to the mass M only of the black hole, the Lense-Thirring acceleration of the order of $O(S/c^2)$ induced by its angular momentum

$$S = \chi \frac{M^2 G}{c}, |\chi| \leq 1 \quad (71)$$

and the one of the order of $O(S^2/c^2)$ due to the hole's quadrupole mass moment

$$Q_2 = -\frac{S^2}{c^2 M}. \quad (72)$$

in the special case in which the hole's spin axis \hat{k} is aligned with the z axis. It may be noted that, in view of Equation (71), the Lense-Thirring acceleration in the field of a Kerr black hole is, actually, of the order of $O(1/c^3)$, while the quadrupolar one is formally Newtonian when Q_2 is introduced.

While the first two accelerations are identical to those arising in the field of a rotating material body of mass M , equatorial radius R and angular momentum S to the first post-Newtonian (1pN) level, i.e. to the order of $\mathcal{O}(1/c^2)$, the latter one corresponds to the purely Newtonian acceleration caused by the body's oblateness J_2 after the formal replacement

$$Q_2 \rightarrow -J_2 MR^2. \quad (73)$$

3.2 The accelerations of the order of $\mathcal{O}(1/c^4)$

In Equations (68)–(70), the acceleration which is formally of the order of $\mathcal{O}(1/c^4)$ consists of the sum of five terms only some of which have directly identifiable equivalents in the case where the primary is a rotating material body. They are the 2pN mass-only acceleration, the acceleration due to the hole's mass multipole of degree $\ell = 4$

$$Q_4 = \frac{S^4}{c^4 M^3}, \quad (74)$$

whose counterpart is the Newtonian acceleration due to the second even zonal harmonic

$$J_4 \rightarrow -\frac{Q_4}{MR^4} \quad (75)$$

of the central material source, and a part of the total acceleration of the order of $\mathcal{O}(S^2/c^4)$, the latter being

$$A_r^{(S^2/c^4)} = \frac{GS^2}{4c^4 Mr^5} \left[-24GM - 9r\dot{r}^2 + 3r^3\dot{\theta}^2 + (-56GM - 27r\dot{r}^2 + 9r^3\dot{\theta}^2) \cos 2\theta - 48r^2\dot{r}\dot{\theta} \cos \theta \sin \theta + 3r^3\dot{\phi}^2 (1 + 3 \cos 2\theta) \sin^2 \theta \right], \quad (76)$$

$$A_\theta^{(S^2/c^4)} = \frac{GS^2}{8c^4 Mr^5} \left\{ -72r^2\dot{r}\dot{\theta} \cos 2\theta + \left[-56GM + 12r\dot{r}^2 + 6r^3(-6\dot{\theta}^2 + \dot{\phi}^2) \right] \sin 2\theta - 3r^2(8\dot{r}\dot{\theta} + r\dot{\phi}^2 \sin 4\theta) \right\}, \quad (77)$$

$$A_\phi^{(S^2/c^4)} = -\frac{3GS^2\dot{\phi} \sin \theta (\dot{r} + 3\dot{r} \cos 2\theta + 2r\dot{\theta} \sin 2\theta)}{c^4 Mr^3}. \quad (78)$$

The aforementioned piece of Equations (76)–(78) corresponding to the 1pN quadrupolar acceleration of the order of $\mathcal{O}(J_2/c^2)$ in the case of an material oblate primary is

$$A^{(J_2/c^2)} = \frac{GMJ_2R^2}{c^2 r^4} \left\{ \frac{3}{2} \left[(5r_k^2 - 1) \hat{r} - 2r_k \hat{k} \right] \left(v^2 - \frac{4GM}{r} \right) - 6 \left[(5r_k^2 - 1) v_r - 2r_k v_k \right] v - \frac{2GM}{r} (3r_k^2 - 1) \hat{r} \right\}. \quad (79)$$

In Equation (79), it is

$$r_k := \hat{\mathbf{r}} \cdot \hat{\mathbf{k}}, \quad (80)$$

$$v_r := \mathbf{v} \cdot \hat{\mathbf{r}}, \quad (81)$$

$$v_k := \mathbf{v} \cdot \hat{\mathbf{k}}. \quad (82)$$

Note that while Equation (80) is dimensionless, Equations (81)–(82) have the dimensions of a speed. The orbital effects due to Equation (79), calculated for any orientations of $\hat{\mathbf{k}}$, can be found in Iorio (2024). Instead, the two terms of the order of $\mathcal{O}(1/c^4)$ which are proportional to S and S^3 do not seem to have any known counterpart where the central object is a material body. Their orbital effects will be worked out in Sections 5 and 7.

About the remaining part of the order of $\mathcal{O}(S^2/c^4)$ which adds to Equation (79) to form the total acceleration of Equations (76)–(78) provided that the replacements of Equations (72)–(73) are made, it is less clear if or to which extent it has possible equivalents in the case of a material source. Its orbital consequences will be treated in Section 6. As it will become clearer there, the explicit form of such a term somehow recalls the acceleration present inside a spinning mass shell (Mashhoon et al., 1984; Pfister and Braun, 1985).

4 The calculational scheme for the orbital effects

The orbital effects of those accelerations of Section 3.2 which have not yet been explicitly investigated in the literature can be calculated with the standard perturbative techniques in terms of the Keplerian orbital elements. They are as follows. The orbit's semimajor axis is⁶ a , $n_K := \sqrt{GM/a^3}$ is the Keplerian mean motion, $P_K = 2\pi/n_K$ is the Keplerian orbital period, e is the eccentricity, $p := a(1 - e^2)$ is the semilatus rectum, I is the inclination of the orbital plane to the fundamental plane Π of the coordinate system adopted, Ω is the longitude of the ascending node⁷, ω is the argument of pericentre, f is the true anomaly, $u := \omega + f$ is the argument of latitude, η is the mean anomaly at epoch, and r is the distance of the test particle from the primary which, in the case of the Keplerian ellipse, is

$$r = \frac{p}{1 + e \cos f}. \quad (83)$$

Furthermore, if \mathbf{A} is any additional acceleration with respect of the Newtonian inverse-square one, it has, first, to be decomposed in three components

$$A_r := \mathbf{A} \cdot \hat{\mathbf{r}}, \quad (84)$$

$$A_\tau = \mathbf{A} \cdot \hat{\boldsymbol{\tau}}, \quad (85)$$

$$A_h = \mathbf{A} \cdot \hat{\mathbf{h}} \quad (86)$$

⁶It should not be confused with the dimensional black hole's spin parameter, usually dubbed a_g as in Equation (10).

⁷It should not be confused with the angular speed Ω of a rotating reference frame and with its gravitational analogue Ω_g of Equation (129).

along the mutually perpendicular radial, transverse and normal directions. The unit vectors of the latter ones are

$$\hat{\mathbf{r}} = \{\cos \Omega \cos u - \cos I \sin \Omega \sin u, \sin \Omega \cos u + \cos I \cos \Omega \sin u, \sin I \sin u\}, \quad (87)$$

$$\hat{\mathbf{\tau}} = \{-\cos \Omega \sin u - \cos I \sin \Omega \cos u, -\sin \Omega \sin u + \cos I \cos \Omega \cos u, \sin I \cos u\}, \quad (88)$$

$$\hat{\mathbf{h}} = \{\sin I \sin \Omega, -\sin I \cos \Omega, \cos I\}. \quad (89)$$

The unit vector $\hat{\mathbf{h}}$ is directed along the orbital angular momentum perpendicularly to the orbital plane.

Then, Equations (84)–(86) must be inserted in the right-hand-sides of the equations for the variations of the orbital elements in the Euler-Gauss form (Brouwer and Clemence, 1961; Soffel, 1989; Bertotti et al., 2003; Brumberg, 1991; Roy, 2005; Kopeikin et al., 2011; Poisson and Will, 2014; Soffel and Han, 2019; Iorio, 2024), which are valid irrespectively of the physical origin of A . They are

$$\frac{da}{dt} = \frac{2}{n_K \sqrt{1-e^2}} \left[e A_r \sin f + \left(\frac{p}{r} \right) A_\tau \right], \quad (90)$$

$$\frac{de}{dt} = \frac{\sqrt{1-e^2}}{n_K a} \left\{ A_r \sin f + A_\tau \left[\cos f + \frac{1}{e} \left(1 - \frac{r}{a} \right) \right] \right\}, \quad (91)$$

$$\frac{dI}{dt} = \frac{1}{n_K a \sqrt{1-e^2}} A_h \left(\frac{r}{a} \right) \cos u, \quad (92)$$

$$\frac{d\Omega}{dt} = \frac{1}{n_K a \sin I \sqrt{1-e^2}} A_h \left(\frac{r}{a} \right) \sin u, \quad (93)$$

$$\frac{d\omega}{dt} = \frac{\sqrt{1-e^2}}{n_K a e} \left[-A_r \cos f + A_\tau \left(1 + \frac{r}{p} \right) \sin f \right] - \cos I \frac{d\Omega}{dt}, \quad (94)$$

$$\frac{d\eta}{dt} = -\frac{2}{n_K a} A_r \left(\frac{r}{a} \right) - \frac{(1-e^2)}{n_K a e} \left[-A_r \cos f + A_\tau \left(1 + \frac{r}{p} \right) \sin f \right]. \quad (95)$$

Finally, after having evaluated their right-hand-sides onto the Keplerian ellipse assumed as reference unperturbed trajectory, the average over one orbital period P_K has to be calculated by means of

$$\frac{dt}{df} = \frac{r^2}{\sqrt{GMp}}, \quad (96)$$

where r is given by Equation (83).

For computational purposes, it is convenient to express the radial and transverse unit vectors of Equations (87)–(88) as

$$\hat{\mathbf{r}} = \hat{\mathbf{l}} \cos u + \hat{\mathbf{m}} \sin u, \quad (97)$$

$$\hat{\mathbf{\tau}} = \hat{\mathbf{m}} \cos u - \hat{\mathbf{l}} \sin u. \quad (98)$$

In them,

$$\hat{\mathbf{l}} := \{\cos \Omega, \sin \Omega, 0\}, \quad (99)$$

$$\hat{\mathbf{m}} := \{-\cos I \sin \Omega, \cos I \cos \Omega, \sin I\} \quad (100)$$

are two mutually perpendicular unit vectors lying in the orbital plane such that $\hat{\mathbf{l}}$ is directed along the line of nodes⁸ towards the ascending node \nearrow . The unit vectors $\hat{\mathbf{l}}, \hat{\mathbf{m}}, \hat{\mathbf{h}}$ form a right-handed orthonormal basis such that $\hat{\mathbf{l}} \times \hat{\mathbf{m}} = \hat{\mathbf{h}}$ holds, as can be directly verified by using Equation (89) and Equations (99)–(100).

It is useful to define also the following auxiliary quantities specifically pertaining the accelerations of Section 3.2:

$$\mathbf{k}\mathbf{l} := \hat{\mathbf{k}} \cdot \hat{\mathbf{l}}, \quad (101)$$

$$\mathbf{k}\mathbf{m} := \hat{\mathbf{k}} \cdot \hat{\mathbf{m}}, \quad (102)$$

$$\mathbf{k}\mathbf{h} := \hat{\mathbf{k}} \cdot \hat{\mathbf{h}}, \quad (103)$$

and

$$\widehat{T}_1 := 1, \quad (104)$$

$$\widehat{T}_2 := \mathbf{k}\mathbf{l}^2 + \mathbf{k}\mathbf{m}^2, \quad (105)$$

$$\widehat{T}_3 := \mathbf{k}\mathbf{l}^2 - \mathbf{k}\mathbf{m}^2, \quad (106)$$

$$\widehat{T}_4 := \mathbf{k}\mathbf{h} \mathbf{k}\mathbf{l}, \quad (107)$$

$$\widehat{T}_5 := \mathbf{k}\mathbf{h} \mathbf{k}\mathbf{m}, \quad (108)$$

$$\widehat{T}_6 := \mathbf{k}\mathbf{l} \mathbf{k}\mathbf{m}. \quad (109)$$

In spherical coordinates, the components of the primary's spin axis $\hat{\mathbf{k}}$, assumed aligned with the reference z axis, are

$$k_r = \cos \theta, \quad (110)$$

$$k_\theta = -\sin \theta, \quad (111)$$

$$k_\phi = 0. \quad (112)$$

Useful dimensionless quantities which will be used in the next Sections are

$$x_s := \frac{a}{r_s},$$

⁸It is the intersection of the orbital plane with the fundamental plane Π of the coordinate system adopted.

where

$$r_s := \frac{2GM}{c^2} \quad (113)$$

is the hole's Schwarzschild radius, and

$$m_\odot := \frac{M}{M_\odot}, \quad (114)$$

where M_\odot is the Sun's mass.

A final remark about the interpretation of the outcome of the aforementioned calculational procedure is in order to avoid possible misunderstandings. Indeed, Equations (90)–(95) return the rates of the contact orbital elements some of which, in general, do not coincide with their osculating counterparts when velocity-dependent accelerations are present (Efroimsky and Goldreich, 2004; Efroimsky, 2005a,b; Kopeikin et al., 2011). Checking explicitly such a subtle feature in the present case is beyond the scope of the present paper.

5 The velocity-dependent acceleration of order $O(S/c^4)$

The components of the velocity-dependent acceleration of the order of $O(S/c^4)$ in spherical coordinates turn out to be

$$A_r^{(S/c^4)} = -\frac{2GS(4GM + 3r\dot{r}^2)\dot{\phi}\sin^2\theta}{c^4r^3}, \quad (115)$$

$$A_\theta^{(S/c^4)} = \frac{6GS\dot{\phi}\sin\theta(2GM\cos\theta - r^2\dot{r}\dot{\theta}\sin\theta)}{c^4r^3}, \quad (116)$$

$$A_\phi^{(S/c^4)} = \frac{GS\{-12GMr\dot{\theta}\cos\theta + \dot{r}[4GM - 3r^3\dot{\phi}^2(1 - \cos 2\theta)]\sin\theta\}}{c^4r^4}. \quad (117)$$

Equations (115)–(117) can be cast into the coordinate-independent vector form

$$A^{(S/c^4)} = \frac{2GS}{c^4} \left\{ \frac{2GM}{r^4} [-3\hat{k} \times \mathbf{v} + 5(\hat{k} \times \mathbf{v} \cdot \hat{r})\hat{r} + 4v_r\hat{k} \times \hat{r}] + \frac{3}{r^3}(\hat{k} \times \mathbf{v} \cdot \hat{r})v_r\mathbf{v} \right\}, \quad (118)$$

valid for an arbitrary orientation of the hole's spin axis \hat{k} in space. The resulting orbital rates of change, averaged over one orbital revolution, are

$$\frac{da}{dt} = 0, \quad (119)$$

$$\frac{de}{dt} = 0, \quad (120)$$

$$\frac{dI}{dt} = -\frac{G^2SM\{e^2\mathbf{k}\mathbf{m}\sin 2\omega + \mathbf{k}\mathbf{l}\left[3(2 + e^2) + e^2\cos 2\omega\right]\}}{c^4a^4(1 - e^2)^{5/2}}, \quad (121)$$

$$\frac{d\Omega}{dt} = -\frac{G^2 S M \left\{ -\mathbf{k}\mathbf{m} \left[-3(2+e^2) + e^2 \cos 2\omega \right] + e^2 \mathbf{k}\mathbf{l} \sin 2\omega \right\}}{c^4 a^4 (1-e^2)^{5/2} \sin I}, \quad (122)$$

$$\frac{d\omega}{dt} = \frac{G^2 S M \left(2(5+e^2) \mathbf{k}\mathbf{h} + \cot I \left\{ -\mathbf{k}\mathbf{m} \left[-3(2+e^2) + e^2 \cos 2\omega \right] + e^2 \mathbf{k}\mathbf{l} \sin 2\omega \right\} \right)}{c^4 a^4 (1-e^2)^{5/2}}, \quad (123)$$

$$\frac{d\eta}{dt} = \frac{6G^2 S M (1+2e^2) \mathbf{k}\mathbf{h}}{c^4 a^4 (1-e^2)^2}. \quad (124)$$

By using Equations (71)–(72), valid for a Kerr black hole, the amplitudes of Equations (119)–(124) turn out to be

$$\frac{d\kappa^{(S/c^4)}}{dt} \propto \frac{c^3 \chi}{16 GM x_s^4} = \frac{\chi}{m_\odot x_s^4} 2.3 \times 10^{13} \text{ deg yr}^{-1}, \quad \kappa = I, \Omega, \omega, \eta, \quad (125)$$

while the shifts per orbit are proportional to

$$\Delta\kappa^{(S/c^4)} \propto \frac{\pi \chi}{2 \sqrt{2} x_s^{5/2}}, \quad \kappa = I, \Omega, \omega, \eta. \quad (126)$$

For $e = 0$, Equation (125) implies that

$$\frac{d\kappa^{(S/c^4)}/dt}{d\kappa^{\text{LT}}/dt} \propto \frac{1}{2x_s}. \quad (127)$$

The Lense-Thirring effect is always larger than its counterpart of the order of $\mathcal{O}(S/c^4)$, as per Equation (127). More precisely, if $e = 0$, in the case of I and Ω , the figure of Equation (127) has to be rescaled by a factor of 3. Indeed, Equations (121)–(122) bring in a scaling factor of 6 for a circular orbit. On the other hand, the corresponding Lense-Thirring amplitudes for the same value of the eccentricity are rescaled by a factor of 2, as per Equations (5.32)–(5.33) of Iorio (2024), being the factors accounting for the spin-orbit configuration equal for both the spin-dependent effects considered. Thus, if $x_s \approx 7$ (Iorio, 2025), as in the case of the disk/jet precession around M87* (Cui et al., 2023), the precessional contribution of the order of $\mathcal{O}(S/c^4)$ would amount to $\approx 21\%$ of the Lense-Thirring effect itself. Since the current accuracy level in measuring the precessional rate in M87*, attributed so far to the Lense-Thirring effect, is $\approx 3\%$ (Cui et al., 2023), it does not seem unrealistic to think that such a novel feature of motion will become detectable in the not too distant future. Essentially the same situation occurs for the recently measured disk/jet precession associated with the tidal disruption event AT2020afhd (Wang et al., 2025), also attributed to the Lense-Thirring effect. Indeed, while its measurement accuracy is of the order of 7% (Wang et al., 2025), on the other hand, it can be shown that the dimensionless radius of the fictitious test particle orbit effectively modeling it is about $x_s \approx 8$, implying that the effect of the order of $\mathcal{O}(S/c^4)$ amounts to $\approx 18\%$ of the Lense-Thirring precession.

6 The position-dependent acceleration of the order of $\mathcal{O}(S^2/c^4)$

The position-dependent part of the acceleration of the order of $\mathcal{O}(S^2/c^4)$ which does not have a counterpart of the order of $\mathcal{O}(J_2/c^2)$ in the case of an oblate material primary may be dubbed as Kerr-only quadrupolar acceleration, or Kerr-only Q_2/c^2 acceleration because of Equation (72). It can be formally

expressed as the sum of two terms apparently resembling a centrifugal and a centripetal acceleration, respectively, as

$$\mathbf{A}^{(S^2/c^2)} = -\boldsymbol{\Omega}_g \times \boldsymbol{\Omega}_g \times \mathbf{r} - \Omega_g^2 \mathbf{r} = -(\boldsymbol{\Omega}_g \cdot \mathbf{r}) \boldsymbol{\Omega}_g, \quad (128)$$

where $\boldsymbol{\Omega}_g$ is given by

$$\boldsymbol{\Omega}_g = \frac{GS}{c^2 r^3} [\hat{\mathbf{k}} - 3(\hat{\mathbf{k}} \cdot \hat{\mathbf{r}}) \hat{\mathbf{r}}]. \quad (129)$$

It is intended that Equation (128) concurs with Equation (79) to form the total acceleration of the order of $\mathcal{O}(S^2/c^4)$ of Equations (76)–(78), which generally depends on the velocity as well. It may be interesting to note that Equation (128) somehow recalls the acceleration experienced by a test particle in the interior of a rotating mass shell (Mashhoon et al., 1984; Pfister and Braun, 1985).

The explicit expressions of the components of Equation (128) in spherical coordinates

$$A_r^{(S^2/c^2)} = -\frac{4G^2 S^2 \cos^2 \theta}{c^4 r^5}, \quad (130)$$

$$A_\theta^{(S^2/c^2)} = \frac{G^2 S^2 \sin 2\theta}{c^4 r^5}, \quad (131)$$

$$A_\phi^{(S^2/c^2)} = 0 \quad (132)$$

elucidate that, in fact, the attributes ‘centrifugal’ and ‘centripetal’ are merely formal. Indeed, it can be noted that it vanishes in the hole’s equatorial plane for $\theta = \pi/2$, while it is directed inward along the rotation axis for $\theta = 0, \pi$.

The resulting orbital rates of change, averaged over one orbital revolution, are

$$\frac{da}{dt} = 0, \quad (133)$$

$$\frac{de}{dt} = -\frac{eG^2 S^2 (\widehat{T}_3 \sin 2\omega - 2\widehat{T}_6 \cos 2\omega)}{4c^4 n_K a^6 (1 - e^2)^2}, \quad (134)$$

$$\frac{dI}{dt} = \frac{G^2 S^2 \{ \widehat{T}_4 [2(2 + e^2) + e^2 \cos 2\omega] + e^2 \widehat{T}_5 \sin 2\omega \}}{4c^4 n_K a^6 (1 - e^2)^3}, \quad (135)$$

$$\frac{d\Omega}{dt} = \frac{G^2 S^2 \{ e^2 \widehat{T}_4 \sin 2\omega + \widehat{T}_5 [2(2 + e^2) - e^2 \cos 2\omega] \}}{4c^4 n_K a^6 \sin I (1 - e^2)^3}, \quad (136)$$

$$\begin{aligned} \frac{d\omega}{dt} = & \frac{G^2 S^2}{8c^4 n_K a^6 (1 - e^2)^3} \{ 6(4 + e^2) \widehat{T}_2 + (2 + 3e^2) \widehat{T}_3 \cos 2\omega - 2e^2 \cot I \widehat{T}_4 \sin 2\omega + \\ & + \cot I \widehat{T}_5 [-4(2 + e^2) + 2e^2 \cos 2\omega] + 2(2 + 3e^2) \widehat{T}_6 \sin 2\omega \}, \end{aligned} \quad (137)$$

$$\frac{d\eta}{dt} = \frac{G^2 S^2 [2(4+5e^2)\widehat{T}_1 + (-2+5e^2)(\widehat{T}_3 \cos 2\omega + 2\widehat{T}_6 \sin 2\omega)]}{8c^4 n_{\text{K}} a^6 (1-e^2)^{5/2}}. \quad (138)$$

By using Equations (71)–(72), valid for a Kerr black hole, the amplitudes of Equations (8.9)–(8.10) in Iorio (2024) and of Equations (133)–(138) turn out to be

$$\frac{d\kappa^{(S^2/c^2)}}{dt} \propto \frac{c^3 \chi^2}{16 \sqrt{2} GM x_s^{9/2}} = \frac{\chi^2}{m_{\odot} x_s^{9/2}} 1.6 \times 10^{13} \text{ deg yr}^{-1}, \quad \kappa = a, e, I, Q, \omega, \eta, \quad (139)$$

while the shifts per orbit are proportional to

$$\Delta\kappa^{(S^2/c^2)} \propto \frac{\pi \chi^2}{4 x_s^3}. \quad (140)$$

For $e = 0$, Equation (139) implies that

$$\frac{d\kappa^{(S^2/c^4)}/dt}{d\kappa^{\text{LT}}/dt} = \frac{\chi}{2 \sqrt{2} x_s^{3/2}}; \quad (141)$$

the Lense-Thirring precessions are even larger than their counterparts of the order of $\mathcal{O}(S^2/c^4)$. In the case of I and Q , the figure of Equation (141) has to be rescaled by a factor of $(11/4)\text{kh}$. Indeed, Equations (8.9)–(8.10) of Iorio (2024) and Equations (135)–(136) bring in an overall scaling factor of $9/2 + 1 = 11/2$ for a circular orbit. On the other hand, the corresponding Lense-Thirring amplitudes for the same value of the eccentricity are rescaled by a factor of 2, as per Equations (5.32)–(5.33) of Iorio (2024). Thus, if $x_s \simeq 7$ (Iorio, 2025), as in the case of the disk/jet precession around M87* (Cui et al., 2023), the total precessional contribution of the order of $\mathcal{O}(S^2/c^4)$ would amount to $\lesssim 5\%$ of the Lense-Thirring effect itself. Since the current accuracy level in measuring the precessional rate in M87*, attributed so far to the Lense-Thirring effect, is $\simeq 3\%$ (Cui et al., 2023), it does not appear impossible that such a feature of motion can be already detectable. Maybe, they will become even better measurable in the not too distant future in view of possible improvements in the measuring accuracy of the disk/jet precession.

7 The velocity-dependent acceleration of order $\mathcal{O}(S^3/c^4)$

The components of the velocity-dependent acceleration of the order of $\mathcal{O}(S^3/c^4)$ in spherical coordinates turn out to be

$$A_r^{(S^3/c^4)} = -\frac{GS^3 \dot{\phi} (3 + 5 \cos 2\theta) \sin^2 \theta}{2c^4 M^2 r^4}, \quad (142)$$

$$A_{\theta}^{(S^3/c^4)} = \frac{GS^3 \dot{\phi} (-2 \sin 2\theta + 5 \sin 4\theta)}{2c^4 M^2 r^4}, \quad (143)$$

$$A_{\phi}^{(S^3/c^4)} = \frac{GS^3 [-4r\dot{\theta} (3 \cos \theta + 5 \cos 3\theta) + 3\dot{r} (\sin \theta + 5 \sin 3\theta)]}{4c^4 M^2 r^5}. \quad (144)$$

Equations (142)–(144) can be cast into the coordinate-independent vector form

$$\mathbf{A}^{(S^3/c^4)} = \frac{3GS^3}{c^4 M^2 r^5} \left[(-1 + 5r_k^2) \hat{\mathbf{k}} \times \mathbf{v} + 5r_k \left(1 - \frac{7}{3} r_k^2 \right) \hat{\mathbf{r}} \times \mathbf{v} \right], \quad (145)$$

valid for an arbitrary orientation of the hole's spin axis $\hat{\mathbf{k}}$ in space. The resulting orbital rates of change, averaged over one orbital revolution, are

$$\frac{da}{dt} = 0, \quad (146)$$

$$\frac{de}{dt} = \frac{15eGS^3\mathbf{k}\mathbf{h}(\widehat{T}_3 \sin 2\omega - 2\widehat{T}_6 \cos 2\omega)}{4c^4M^2a^5(1-e^2)^{5/2}}, \quad (147)$$

$$\begin{aligned} \frac{dI}{dt} = & -\frac{3GS^3}{8c^4M^2a^5(1-e^2)^{7/2}} \{2(2+3e^2)\mathbf{k}\mathbf{l}(-4+5\widehat{T}_2) + \\ & + 5e^2[\mathbf{k}\mathbf{l}(-2+3\mathbf{k}\mathbf{l}^2+\mathbf{k}\mathbf{m}^2)\cos 2\omega + 2\mathbf{k}\mathbf{m}(-1+2\mathbf{k}\mathbf{l}^2+\mathbf{k}\mathbf{m}^2)\sin 2\omega]\}, \end{aligned} \quad (148)$$

$$\begin{aligned} \frac{d\Omega}{dt} = & -\frac{3GS^3}{8c^4M^2a^5(1-e^2)^{7/2}\sin I} \{2(2+3e^2)\mathbf{k}\mathbf{m}(-4+5\widehat{T}_2) + \\ & + 5e^2[-\mathbf{k}\mathbf{m}(-2+\mathbf{k}\mathbf{l}^2+3\mathbf{k}\mathbf{m}^2)\cos 2\omega + 2\mathbf{k}\mathbf{l}(-1+\mathbf{k}\mathbf{l}^2+2\mathbf{k}\mathbf{m}^2)\sin 2\omega]\}, \end{aligned} \quad (149)$$

$$\begin{aligned} \frac{d\omega}{dt} = & \frac{3GS^3}{8c^4M^2a^5(1-e^2)^{7/2}} \{4(3+2e^2)\mathbf{k}\mathbf{h}(-2+5\widehat{T}_2) + 2(2+3e^2)\mathbf{k}\mathbf{m}(-4+5\widehat{T}_2)\cot I + \\ & + 5\cos 2\omega[2(1+2e^2)\mathbf{k}\mathbf{h}\widehat{T}_3 - e^2\mathbf{k}\mathbf{m}(-2+\mathbf{k}\mathbf{l}^2+3\mathbf{k}\mathbf{m}^2)\cot I] + \\ & + 10\mathbf{k}\mathbf{l}[2(1+2e^2)\widehat{T}_5 + e^2(-1+\mathbf{k}\mathbf{l}^2+2\mathbf{k}\mathbf{m}^2)\cot I]\sin 2\omega\}, \end{aligned} \quad (150)$$

$$\frac{d\eta}{dt} = -\frac{3GS^3\mathbf{k}\mathbf{h}[5\widehat{T}_3\cos 2\omega + 2(-2+5\widehat{T}_2+5\widehat{T}_6\sin 2\omega)]}{4c^4M^2a^5(1-e^2)^2}. \quad (151)$$

By using Equations (71)–(72), valid for a Kerr black hole, the amplitudes of Equations (146)–(151) turn out to be

$$\frac{d\kappa^{(S^3/c^4)}}{dt} \propto \frac{c^3\chi^3}{32GMx_s^5} = \frac{\chi^3}{m_\odot x_s^5} 1.1 \times 10^{13} \text{ deg yr}^{-1}, \quad \kappa = I, \Omega, \omega, \eta, \quad (152)$$

while the shifts per orbit are proportional to

$$\Delta\kappa^{(S^3/c^4)} \propto \frac{\pi\chi^3}{4\sqrt{2}x_s^{7/2}}, \quad \kappa = I, \Omega, \omega, \eta. \quad (153)$$

For $e = 0$, Equation (152) implies that

$$\frac{d\kappa^{(S^3/c^4)}/dt}{d\kappa^{\text{LT}}/dt} \propto \frac{\chi^2}{4x_s^2}. \quad (154)$$

From Equation (154) it turns out that the precessions of the order of $\mathcal{O}(S^3/c^4)$ are quite smaller than the Lense-Thirring ones. Thus, it is difficult but not impossible that such features of motion can play a role in the interpretation of the observations of disk/jet precessions around supermassive black holes.

8 The impact on the M87* disk/jet precession

The disk/jet coprecession around M87* was recently detected to a $\simeq 3\%$ accuracy (Cui et al., 2023). In particular, its measured precessional angular speed Ω_p turned out to be (Cui et al., 2023)

$$\Omega_p^{\text{meas}} = 0.56 \pm 0.02 \text{ rad yr}^{-1} = 32 \pm 1 \text{ deg yr}^{-1}. \quad (155)$$

It was recently shown that Equation (155) can be reproduced by the Lense-Thirring precessional angular speed of the orbital angular momentum of a fictitious test particle moving along an effective inclined and circular orbit at about 14 gravitational radii from the central black hole (Iorio, 2025). The precession of Equation (89) is directly related to the rates of change of the inclination I and the node Ω through

$$\frac{d\hat{\mathbf{h}}}{dt} = \frac{\partial \hat{\mathbf{h}}}{\partial I} \frac{dI}{dt} + \frac{\partial \hat{\mathbf{h}}}{\partial \Omega} \frac{d\Omega}{dt} = \boldsymbol{\Omega}_p \times \hat{\mathbf{h}}. \quad (156)$$

In Equation (156), the theoretical angular velocity $\boldsymbol{\Omega}_p$ can be calculated from the expressions of dI/dt and $d\Omega/dt$ for each of the accelerations considered in the previous Sections. Figures 1 to 2 display the allowed regions in the two-dimensional parameter space spanned by the dimensionless spin parameter of M87*, here dubbed a^* , and the effective radius r_0 , in units of gravitational radii, of the orbit of the fictitious test particle. They were obtained as in Iorio (2025), namely by imposing that the absolute value of the analytically computed theoretical precessional frequencies, considered as functions of a^* and r_0 , is constrained by the experimental range of Equation (155).

It can be noticed that, for positive values of a^* , the inclusion of the contributions of the order of $\mathcal{O}(S/c^4)$ and, to a lesser extent, of $\mathcal{O}(S^2/c^4)$ as well, change the allowed regions in a non-negligible way, leading generally to smaller permitted values of r_0 . The further addition of the term of the order of $\mathcal{O}(S^3/c^4)$ has an almost negligible impact, while the formally Newtonian term proportional to Q_4 has virtually no effect at all. The negative values of a^* yield to a generally different pattern of the allowed regions implying larger values of r_0 . Furthermore, for $|a^*| \simeq 0.9 - 1$, all the permitted domains tend to overlap apart from the one obtained by including only the Lense-Thirring and the quadrupolar terms.

9 Summary and overview

The Kerr metric describing the exterior spacetime of a spinning black hole was written by explicitly expressing the Boyer-Lindquist coordinates $x_{\text{BL}}^0, r_{\text{BL}}, \theta_{\text{BL}}, \phi_{\text{BL}}$ as functions of the harmonic ones x^0, r, θ, ϕ . Exact expressions for the spacetime metric tensor in terms of the latter ones were, thus, obtained. By expanding $g_{\mu\nu}$ in powers of the two characteristic lengths R_g and a_g of the Kerr metric proportional to the hole's mass M and angular momentum S , respectively, approximated formulas for the metric coefficients were derived and used to calculate the geodesic equations of motion of an uncharged, spinless body orbiting the hole at some gravitational radii. Accelerations formally up to the 2pN order were calculated and displayed in a coordinate-independent, vector form valid for any orientations of the hole's spin axis $\hat{\mathbf{k}}$ in space and suitable for practical applications.

Those of the order of $\mathcal{O}(1/c^2)$ are the position-dependent, formally Newtonian acceleration induced by the mass quadrupole moment of the primary, and the velocity-dependent Schwarzschild-like, mass-only and Lense-Thirring accelerations, respectively. They are identical to their counterparts arising in the field of an rotating material body endowed with axial symmetry.

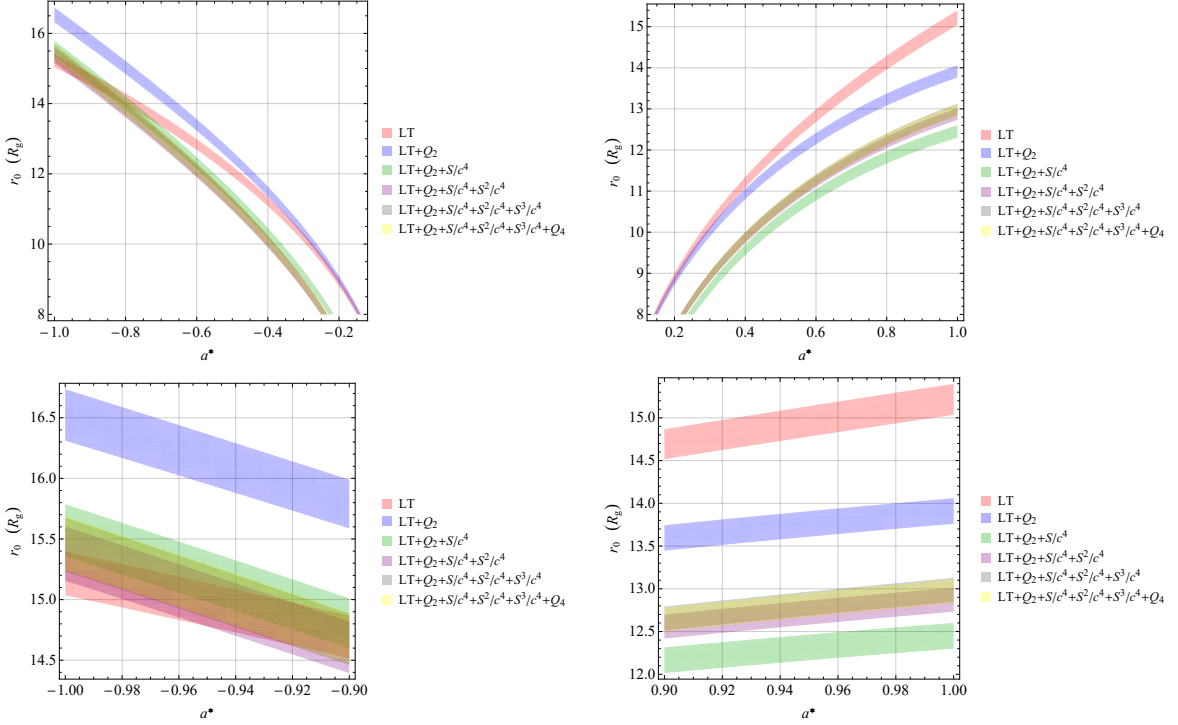


Figure 1: Allowed regions in the $\{a^*, r_0\}$ parameter space of M87* obtained by imposing that the absolute values of the theoretical frequencies of the precession of the orbital plane of a fictitious test particle moving along a tilted, circular effective orbit around the supermassive black hole lie within the experimental range of Equation (155). The labels ‘LT’, ‘ Q_2 ’ and ‘ Q_4 ’ denote the standard Lense-Thirring and the formally Newtonian even zonal harmonic frequencies of degree $\ell = 2, 4$, respectively, while ‘ S/c^4 ’, ‘ S^2/c^4 ’, and ‘ S^3/c^4 ’ refer to the contributions proportional to S/c^4 , S^2/c^4 (the total one) and S^3/c^4 , respectively. See Figure 2 for an overview of all permitted regions.

To the order of $O(1/c^4)$, there are five accelerations. One of them is the known velocity-dependent 2pN mass-only term. The acceleration of the order of $O(S^2/c^2)$ can be formally split as the sum of three components. One of them corresponds to the velocity-dependent 1pN quadrupolar acceleration of the order of $O(J_2/c^2)$ caused by an oblate material body endowed with dimensionless quadrupole mass moment J_2 . Instead, the other two position-dependent components formally resemble to a centrifugal and a centripetal acceleration in an accelerated rotating frame whose angular velocity vector Ω_g is, however, a non-uniform, position-dependent vector field. The position-dependent acceleration proportional to S^4/c^4 formally corresponds to the Newtonian one due to the second even zonal harmonic multipole J_4 of an axisymmetric material primary. Finally, apparently without a counterpart in the case of a material body, one finds two velocity-dependent accelerations proportional to S/c^4 and S^3/c^4 , respectively.

The long-term rates of change of the Keplerian orbital elements induced by the accelerations of the order of $O(S/c^4)$, $O(S^3/c^4)$ and by the one of the order of $O(S^2/c^4)$ sourced by Ω_g were analytically calculated with standard perturbative techniques. The resulting expressions, averaged over one orbital revolution, are not restricted to any values of the particle’s eccentricity e and inclination I , and the hole’s spin axis \hat{k} retains a general orientation in space.

It turned out that the effects of the order of $O(S/c^4)$ may be measurable by exploiting the disk/jet coprecessions around supermassive black holes in galactic nuclei, recently measured to a few per cent accuracy as in the case of M87* and the tidal disruption event AT2020afhd. Indeed, it was demonstrated

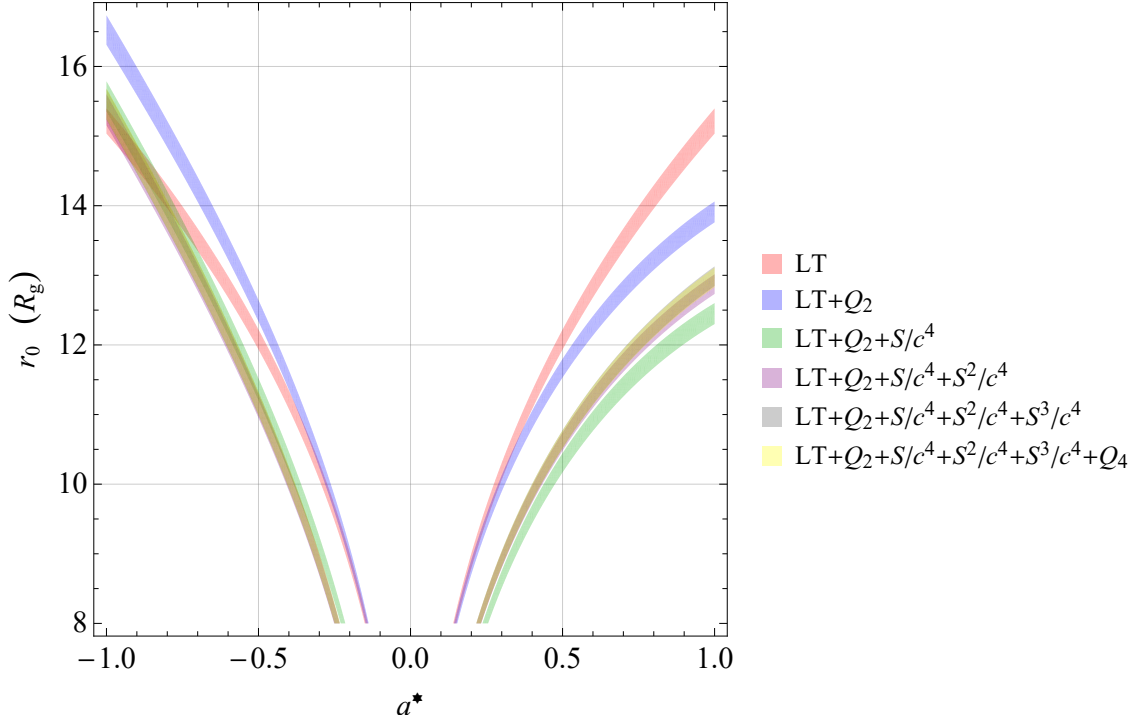


Figure 2: Joint representation of all the allowed regions in the $\{a^*, r_0\}$ parameter space of M87* obtained by imposing that the absolute values of the theoretical frequencies of the precession of the orbital plane of a fictitious test particle moving along a tilted, circular effective orbit around the supermassive black hole lie within the experimental range of Equation (155). The labels ‘LT’, ‘ Q_2 ’ and ‘ Q_4 ’ denote the standard Lense-Thirring and the formally Newtonian even zonal harmonic frequencies of degree $\ell = 2, 4$, respectively, while ‘ S/c^4 ’, ‘ S^2/c^4 ’ and ‘ S^3/c^4 ’ refer to the contributions proportional to S/c^4 , S^2/c^4 (the total one) and S^3/c^4 , respectively.

that such a phenomenology can be explained in terms of the Lense-Thirring precession of the orbital angular momentum of a fictitious test particle moving at about fifteen gravitational radii from the central black hole. To this aim, the precession induced by the aforementioned acceleration proportional to S/c^4 amounts to about twenty per cent of the measured one, assumed due to the Lense-Thirring effect. Also the total precession of the order of S^ϵ/J^Δ is measurable, although to a lesser extent. Instead, the contribution of the order of $O(S^3/c^4)$ is marginally detectable, if any, while the formally Newtonian one induced by the second even zonal harmonic of the primary is negligible. Such conclusions were graphically confirmed by the displayed allowed domains in the two-dimensional parameter space of the jet precession around M87* spanned by the spin parameter of the latter and the effective orbital radius of the fictitious test particle representing the accretion disk.

Data availability

No new data were generated or analysed in support of this research.

Conflict of interest statement

I declare no conflicts of interest.

Funding

This research received no external funding.

Acknowledgements

References

B. Bertotti, P. Farinella, and D. Vokrouhlický. *Physics of the Solar System*. Kluwer, 2003. doi: 10.1007/978-94-010-0233-2.

D. Brouwer and G. M. Clemence. *Methods of Celestial Mechanics*. Academic Press, 1961.

V. A. Brumberg. *Essential Relativistic Celestial Mechanics*. Adam Hilger, 1991.

Y. Cui, K. Hada, T. Kawashima, M. Kino, W. Lin, Y. Mizuno, H. Ro, M. Honma, K. Yi, J. Yu, J. Park, W. Jiang, Z. Shen, E. Kravchenko, J.-C. Algaba, X. Cheng, I. Cho, G. Giovannini, M. Giroletti, T. Jung, R.-S. Lu, K. Niinuma, J. Oh, K. Ohsuga, S. Sawada-Satoh, B. W. Sohn, H. R. Takahashi, M. Takamura, F. Tazaki, S. Trippe, K. Wajima, K. Akiyama, T. An, K. Asada, S. Buttaccio, D.-Y. Byun, L. Cui, Y. Hagiwara, T. Hirota, J. Hodgson, N. Kawaguchi, J.-Y. Kim, S.-S. Lee, J. W. Lee, J. A. Lee, G. Maccaferri, A. Melis, A. Melnikov, C. Migoni, S.-J. Oh, K. Sugiyama, X. Wang, Y. Zhang, Z. Chen, J.-Y. Hwang, D.-K. Jung, H.-R. Kim, J.-S. Kim, H. Kobayashi, B. Li, G. Li, X. Li, Z. Liu, Q. Liu, X. Liu, C.-S. Oh, T. Oyama, D.-G. Roh, J. Wang, N. Wang, S. Wang, B. Xia, H. Yan, J.-H. Yeom, Y. Yonekura, J. Yuan, H. Zhang, R. Zhao, and W. Zhong. Precessing jet nozzle connecting to a spinning black hole in M87. *Nature*, 621:711–715, 2023. doi: 10.1038/s41586-023-06479-6.

M. Efroimsky. Long-Term Evolution of Orbits About A Precessing Oblate Planet: 1. The Case of Uniform Precession. *Celest. Mech. Dyn. Astr.*, 91:75–108, 2005a. doi: 10.1007/s10569-004-2415-z.

M. Efroimsky. Gauge Freedom in Orbital Mechanics. *Ann. N. Y. Acad. Sci.*, 1065:346–374, 2005b. doi: 10.1196/annals.1370.016.

M. Efroimsky and P. Goldreich. Gauge freedom in the N-body problem of celestial mechanics. *Astron. Astrophys.*, 415:1187–1199, 2004. doi: 10.1051/0004-6361:20034058.

S. Herkt and G. Schäfer. Higher-order-in-spin interaction Hamiltonians for binary black holes from source terms of Kerr geometry in approximate ADM coordinates. *Phys. Rev. D*, 77:104001, 2008. doi: 10.1103/PhysRevD.77.104001.

S. Herkt, A. Shah, and G. Schäfer. Observables of a Test Mass along an Inclined Orbit in a Post-Newtonian-Approximated Kerr Spacetime Including the Linear and Quadratic Spin Terms. *Phys. Rev. Lett.*, 111:021101, 2013. doi: 10.1103/PhysRevLett.111.021101.

L. Iorio. *General Post-Newtonian Orbital Effects From Earth's Satellites to the Galactic Center*. Cambridge University Press, 2024. doi: 10.1017/9781009562911.

L. Iorio. Lense-Thirring effect at work in M87*. *Phys. Rev. D*, 111:044035, 2025. doi: 10.1103/PhysRevD.111.044035.

S. M. Kopeikin, M. Efroimsky, and G. Kaplan. *Relativistic Celestial Mechanics of the Solar System*. Wiley, 2011. doi: 10.1002/9783527634569.

B. Mashhoon, F. W. Hehl, and D. S. Theiss. On the gravitational effects of rotating masses: The Thirring–Lense papers. *Gen. Relativ. Gravit.*, 16:711–750, 1984. doi: 10.1007/BF00762913.

H. Pfister and K. H. Braun. Induction of correct centrifugal force in a rotating mass shell. *Class. Quantum Gravit.*, 2:909–918, 1985. doi: 10.1088/0264-9381/2/6/015.

E. Poisson and C. M. Will. *Gravity. Newtonian, Post–Newtonian, Relativistic*. Cambridge University Press, 2014. doi: 10.1017/CBO9781139507486.

R. A. Porto and I. Z. Rothstein. Spin(1)spin(2) effects in the motion of inspiralling compact binaries at third order in the post-Newtonian expansion. *Phys. Rev. D*, 78:044012, 2008. doi: 10.1103/PhysRevD.78.044012.

A. E. Roy. *Orbital Motion. Fourth Edition*. IOP Publishing, 2005.

M. H. Soffel. *Relativity in Astrometry, Celestial Mechanics and Geodesy*. Springer, 1989. doi: 10.1007/978-3-642-73406-9.

M. H. Soffel and W.-B. Han. *Applied General Relativity*. Astronomy and Astrophysics Library. Springer, 2019. doi: 10.1007/978-3-030-19673-8.

Y. Wang, Z. Lin, L. Wu, W. Lei, S. Wei, S.-N. Zhang, L. Ji, S. del Palacio, R. D. Baldi, Y. Huang, J. Liu, B. Zhang, A. Yang, R. Chen, Y. Zhang, A. Wang, L. Yang, P. Charalampopoulos, D. R. A. Williams-Baldwin, Z.-H. Yao, F.-G. Xie, D. Bu, H. Feng, X. Cao, H. Wu, W. Li, E. Qiao, G. Leloudas, J.P. Anderson, X. Shu, D.R. Pasham, H. Zou, M. Nicholl, T. Wevers, T. E. Muller-Bravo, J. Wang, J. Wei, Y.-L. Qiu, W. Guo, C. P. Gutierrez, M. Gromadzki, C. Inserra, L. Makrygianni, F. Onori, T. Petrushevska, D. Altamirano, L. Galbany, M. Perez-Torres, and T.-W. Chen. Detection of disk-jet co-precession in a tidal disruption event. *Science*, 11:eady9068, 2025. doi: 10.1126/sciadv.ady9068.